Supermetal: SbF_5-Mediated Methane Oxidation Occurs by C-H Activation and Isobutane Oxidation Occurs by Hydride Transfer

Journal:	*Dalton Transactions*
Manuscript ID	DT-ART-09-2019-003564.R1
Article Type:	Paper
Date Submitted by the Author:	21-Oct-2019
Complete List of Authors:	King, Clinton; Brigham Young University, Department of Chemistry and Biochemistry Holdaway, Ashley; Brigham Young University, Department of Chemistry and Biochemistry Durrant, George; Brigham Young University, Department of Chemistry and Biochemistry Wheeler, Josh; Brigham Young University, Department of Chemistry and Biochemistry Suaava, Lorna; Brigham Young University, Department of Chemistry and Biochemistry Konnick, Mike; Scripps Florida Periana, Roy; The Scripps Research Institute, Chemistry Ess, Daniel; Brigham Young University, Department of Chemistry and Biochemistry

ARTICLE

Supermetal: SbF_5-Mediated Methane Oxidation Occurs by C-H Activation and Isobutane Oxidation Occurs by Hydride Transfer

Received 00th January 20xx,
Accepted 00th January 20xx

DOI: 10.1039/x0xx00000x

Clinton R. King,[a] Ashley Holdaway,[a] George Durrant,[a] Josh Wheeler,[a] Lorna Suaava,[a] Michael M. Konnick,[b] Roy A. Periana,*[c] and Daniel H. Ess*[a]

Sb^VF_5 is generally assumed to oxidize methane through a methanium-to-methyl cation mechanism. However, experimentally no H_2 is observed, and the mechanism of methane oxidation has remained unsolved for several decades. To solve this problem, density functional theory calculations with multiple chemical models (mononuclear and dinuclear) were used to examine methane oxidation by Sb^VF_5 in the presence of CO leading to the methyl acylium cation ($[CH_3CO]^+$). While there is a low barrier for methane protonation by $[Sb^VF_6]^-[H]^+$ (the combination of Sb^VF_5 and HF) to give the $[Sb^VF_5]^-[CH_5]^+$ ion pair, H_2 dissociation is a relatively higher energy process, even with CO assistance, and so this protonation pathway is reversible. While Sb-mediated hydride transfer has a reasonable barrier, the C-H activation/σ-bond metathesis mechanism with formation of an Sb^V-Me intermediate is lower in energy. This pathway leads to the acylium cation by functionalization of the Sb^V-Me intermediate with CO, and is consistent with no observation of H_2. Because this C-H activation/metal-alkyl functionalization pathway is higher in energy than methane protonation it is also consistent with the experimentally observed hydrogen-to-deuterium exchange in methane. This is the first time that evidence is presented demonstrating that Sb^VF_5 acts beyond a superacid and involves C-H activation with an organometallic intermediate. In contrast to methane, due to the much lower carbocation hydride affinity, isobutane significantly favors hydride transfer to give *tert*-butyl carbocation with concomitant Sb^V to Sb^{III} reduction. In this mechanism, the resulting highly acidic Sb^V-H intermediate provides a route to H_2 through protonation of isobutane, which is consistent with experiments and resolves the longstanding enigma of different experimental results for methane versus isobutane.

Introduction

Reaction of methane with Sb^VF_5, especially in the presence of a Brønsted acid (e.g HF or HSO_3F), is assumed to induce reversible formation of methanium ($[CH_5]^+$) that fragments to H_2 and methyl cation (Scheme 1a), which can further react leading to alkane oligomerization.[1] For methane, the first step of this superacid-induced reaction pathway is supported by the experimental observation of methane hydrogen-to-deuterium (H/D) exchange.[2-4] However, density functional theory (DFT) studies reported competitive low energy transition-state structures for alkane protonation and concerted hydrogen exchange, and both pathways can account for H/D exchange in methane.[5-8] The second step in the methanium-to-methyl cation pathway is tenuous because H_2 is generally not observed.[1,9] However, H_2 is observed for larger alkanes, such as isobutane, although typically in less than stoichiometric amount.[10-16]

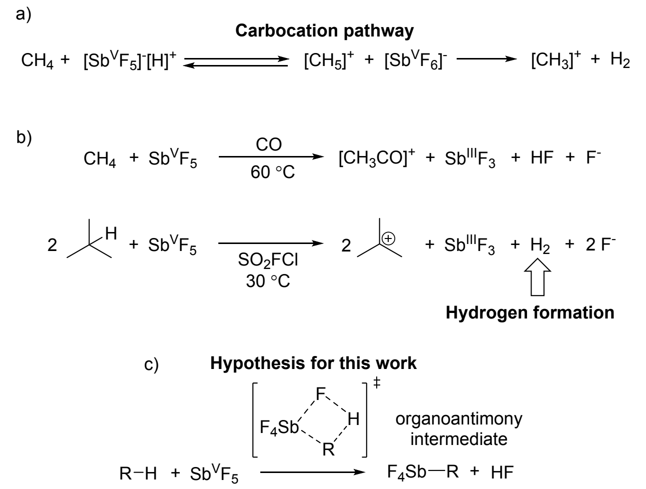

Scheme 1. a) Outline of methyl cation pathway for reaction of methane with $[Sb^VF_6]^-[H]^+$. b) Overview of methane and isobutane oxidation reactions with Sb^VF_5. c) Possible C-H activation transition state and organoantimony intermediate as the first mechanistic step for the oxidation of alkanes by Sb^VF_5.

There are several reasons to explore possible alternative mechanisms for reaction of methane with Sb^VF_5, in particular for conditions without excess Brønsted acid. Hogeveen[17] and de Rege[18] reported that the reaction of methane with neat

---

[a] *Department of Chemistry and Biochemistry, Brigham Young University, Provo, Utah 84602. E-mail: dhe@chem.byu.edu.*
[b] *Hyconix, Inc., 4575 Weaver Pkwy, Warrenville, IL 60555.*
[c] *Department of Chemistry, The Scripps Research Institute, Jupiter, Florida 33458. E-mail: rperiana@scripps.edu.*

Electronic Supplementary Information (ESI) available: Supplemental simulation details and plots. See DOI: 10.1039/x0xx00000x

Sb^VF_5 in the presence of CO at 60 and 80 °C led to formation of methyl acylium cation ($[CH_3CO]^+$) and reduced Sb^{III} with no observation of H_2 (Scheme 1b). Experiments also showed that while H_2 is capable of reducing Sb^V to Sb^{III}, under these conditions the rate of reduction is inconsistent with its formation and rapid reaction without observation.[18] This suggests that the methanium to methyl cation pathway outlined in Scheme 1a is an unlikely route to $[CH_3CO]^+$. Additionally, the relatively mild conditions of this reaction are inconsistent with the ~40 kcal mol^{-1} energy required to dissociate H_2 from methanium.[19,20]

In contrast to the methane reaction, Sommer reported that the reaction of isobutane with neat Sb^VF_5 results in $Sb^{III}F_3$ with observation of both H_2 and *tert*-butyl cation.[13-15] While this result would seemingly fit with a protonation-induced carbocation pathway, Sommer used acetone as a Brønsted base to demonstrate that the small quantity of protons in Sb^VF_5 are unlikely to be involved with the Sb^V to Sb^{III} reduction. Alternative to a carbocation pathway is a pathway that involves direct hydride transfer from isobutane to Sb. However, Olah and others dismissed this pathway with citation of the formation of a very weak Sb-H bond, and unfavourable thermodynamics.[4]

While previous DFT studies examined reaction pathways for H/D exchange by Sb^VF_5 superacids, there has been no computational consideration of mechanisms involving C-H activation/metalation (Scheme 1c) or hydride transfer that provide a route for Sb^V to Sb^{III} reduction. The possibility of C-H activation with an alkylantimony (Sb-R) intermediate is intriguing because the most prominent examples of C-H activation involve transition-metal complexes, and only recently has the possibility of p-block, main-group metals facilitating C-H activation been suggested.[21]

Here we report DFT calculations that compare C-H activation, hydride transfer, and protonation pathways for oxidation of methane and isobutane with Sb^VF_5. We found that the Sb^VF_5-mediated C-H activation pathway is viable and results in an Sb^V-Me intermediate, which can be functionalized by CO resulting in $[CH_3CO]^+$ and Sb^{III}. Because methyl cation is very unstable, this C-H activation pathway is lower in energy than hydride transfer and protonation pathways. In contrast, for isobutane, the hydride transfer transition pathway is a significantly lower energy route than C-H activation, which leads to *tert*-butyl cation and an Sb^V-H intermediate that provides a pathway to H_2 formation.

Methodology

Sb^VF_5 contains small quantities of HF, and protons are produced in the reaction with methane. Therefore, reaction pathways were referenced to the ground state of $[Sb^VF_6]^-[H]^+$ (and $[Sb^V{}_2F_{11}]^-[H]^+$ for a dinuclear model). This refers to the ion pair that forms with coordination of HF to Sb^VF_5. See the Supporting Information (SI) for discussion of alternative possible ground states, such as $F_5Sb^V(CO)$ and $F_5Sb^V(CH_4)$. Dinér[8] used a similar ground state, and this is consistent with Estevez et al's[5-7] previous DFT reports examining plausible structures for the combination of Sb^VF_5 and HF. Because of the limited quantity of HF in Sb^VF_5 we did not use the $[Sb^VF_6]^-[H_2F]^+$ model, which was identified by Kim and Klein's Car-Parrinello molecular dynamics simulations.[22-25] Importantly, this ground state allowed direct comparison of protonation and Sb-mediated reaction pathways.

We used M06/Def2-TZVPDD[26-28]//M06/6-31+G**[LANL2DZdp[29,30] for Sb][31] in Gaussian 09[32] to optimize all minima and transition-state structures, and energies correspond to 298 K. We also compared M06 energies with ωB97X-D and MN15 energies, and the aug-cc-pVTZ basis set. These functionals gave very similar results to M06. Free energies are the sum of $E_{(SCF,Def2\text{-}TZVPDD)} + E_{ZPE(6\text{-}31G^{**}[LANL2DZdp])} + U_{(6\text{-}31G^{**}[LANL2DZdp])} + nRT - TS_{(6\text{-}31G^{**}[LANL2DZdp])} + \Delta G_{solv(Def2\text{-}TZVPDD)}$. Because the isobutane reaction was carried out in SO_2FCl, as an approximation for bulk solvent effects, particularly dielectric stabilization, we used the SMD continuum solvent model for dimethylsulfoxide. Structures were optimized in this continuum model. While this approach is crude, inclusion of solvent-induced electrostatic stabilization is important because hydride transfer and protonation pathways transition states develop significant charge. We also used this continuum solvent model for the methane oxidation reaction, however, because this reaction was reported in neat Sb^VF_5, we also report relevant gas phase values, which is similar to nearly all previous DFT studies that examined Sb^VF_5.

Results and discussion

Protonation and Hydride Transfer Pathways

We began by examining the methanium pathway outlined in Scheme 1a. With $[Sb^VF_6]^-[H]^+$ (the ion pair from HF coordination to Sb^VF_5) as the ground state, we located the methane protonation transition state, **TS1** (Scheme 2a,d). This transition state was previously reported by Dinér, and our intrinsic reaction coordinate (IRC) calculation shows it connects to the $[Sb^VF_6]^-[CH_5]^+$ ion pair. Our M06 $\Delta G^\ddagger$ value is 15.3 kcal mol^{-1} ($\Delta H^\ddagger$ = 5.7 kcal mol^{-1}). This relatively low barrier for protonation is consistent with Raugei and Klein's molecular dynamics study of reaction of light alkanes with Sb^VF_5 in HF that identified highly reactive protons and low barriers for alkane protonation resulting from coordination of HF to Sb^VF_5.[24,25] While there is a low barrier for methane protonation (see the SI for comparison to the one-step hydrogen exchange transition state),[3] even with the solvent stabilization, H_2 dissociation is unlikely. The ΔG to achieve separated $[Sb^VF_6]^-$, $[CH_3]^+$, and H_2 is 53.3 kcal mol^{-1}, and our estimate for achieving $[Sb^VF_6]^-[CH_3]^+$ and H_2 is ~42 kcal mol^{-1} (see SI for discussion about this estimate). This relatively large value for H_2 separation from $[CH_5]^+$ is consistent with Dinér's[8] previously calculated value and the experimentally measured gas phase value of ~40 kcal mol^{-1}.[33]

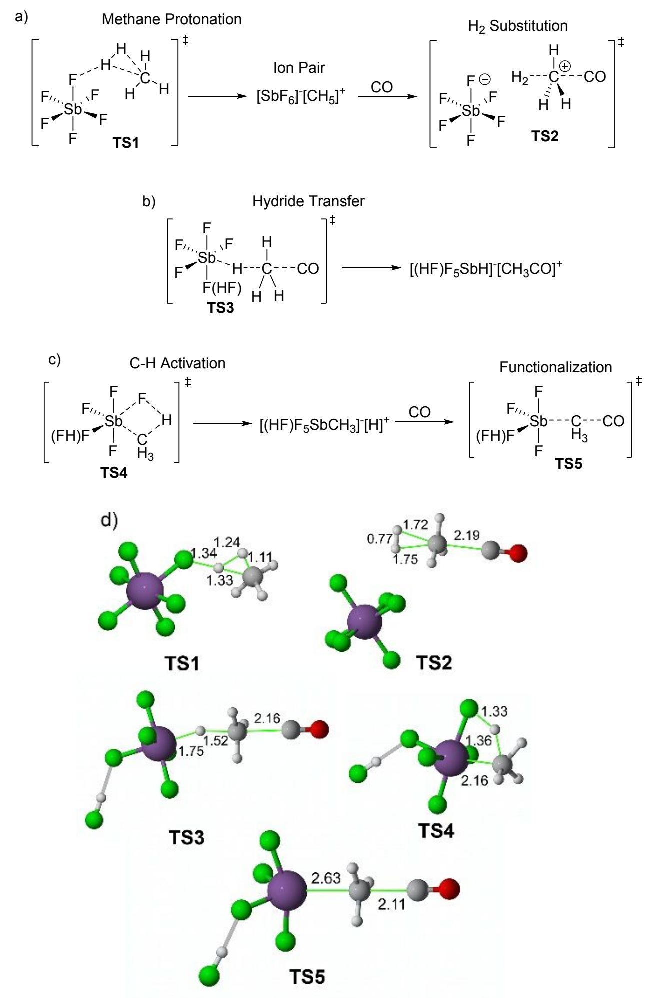

Scheme 2. a) Calculated methyl cation pathway that begins with the methane protonation transition state **TS1**. b) Calculated hydride transfer with simultaneous CO capture of methyl cation. c) C-H activation and CO functionalization transition states. d) 3D depictions of **TS1**-**TS5**.[34]

With our best estimates indicating the formation of methyl cation to be unlikely, we considered pathways that circumvent this high-energy intermediate. Therefore, we examined CO induced H_2 displacement from $[Sb^VF_6]^-[CH_5]^+$ through transition state **TS2** (Scheme 2a). This transition state provides H_2 and the $[CH_3CO]^+[Sb^VF_6]^-$ ion pair. This pathway is only slightly lower in energy than H_2 dissociation from $[Sb^VF_6]^-[CH_5]^+$ with a $\Delta G^‡$ of 49.3 kcal mol^{-1}, which suggests that H_2 dissociation is not feasible. We also located a transition state similar to **TS2**, but with $[Sb^VF_6]^-$ displacing H_2, which was higher in energy than **TS2**. This suggests that methane protonation occurs to achieve $[Sb^VF_6]^-[CH_5]^+$, but that this ion pair is impeded from losing H_2 and this is unlikely to be a productive avenue for formation of $[CH_3CO]^+$ (Scheme 3 pathway), which is consistent with both the experimentally observed H/D exchange in methane and lack of observed H_2.

With the protonation pathway unlikely to account for formation of $[CH_3CO]^+$, we then explored Sb-mediated hydride transfer, which could then undergo reductive elimination to give $Sb^{III}F_3$ and HF. See the SI for details of reaction pathways for hydrogen atom transfer (HAT), electron transfer (ET), and proton-coupled electron transfer (PCET) pathways, which are less viable than hydride transfer. While Hogeveen suggested the possibility of a hydride transfer mechanism between alkanes and Sb^VF_5,[11,17] this mechanism was dismissed by Olah.[4] However, this type of mechanism is generally proposed for carbocation formation for reaction between Sb^VF_5 and alkyl fluorides.[35] For methane, hydride abstraction of methane by Sb^VF_5 requires $\Delta G^‡$ = 56.9 kcal mol^{-1} ($\Delta H^‡$ = 45.3 kcal mol^{-1}) and gives the $[(HF)F_5SbH]^-[CH_3]^+$ ion pair. While this relatively large barrier for hydride abstraction is perhaps not unexpected based on the hydride affinity of methyl cation (>300 kcal mol^{-1}),[36] we examined if hydride transfer would be more feasible if facilitated by CO leading to overall hydride substitution. **TS3** (Scheme 2b,d) with a relatively bent Sb-H-C angle and highly stretched C-H partial bond length provides a one-step route to $[(HF)F_5Sb^VH]^-[CH_3CO]^+$. This transition-state assembly would be preceded by a weak association complex between methane and Sb. Indeed, the presence of CO does lower the hydride transfer barrier to $\Delta G^‡$ = 41.0 kcal mol^{-1} and $\Delta H^‡$ = 33.1 kcal mol^{-1}. However, the >40 kcal mol-1 $\Delta G^‡$ value is unlikely to account for reactivity at 60 or 80 °C. Also, if $[(HF)F_5Sb^VH]^-$ were to be formed it would likely generate H_2 or transfer the hydride to $[CH_3CO]^+$ to give acetaldehyde. Consistent with this argument, the calculated barrier for protonation of $[(HF)F_5SbH]^-$ with HF is 50.7 kcal mol^{-1}, indicating that an Sb^V-H bond is highly acidic.

Sb-Mediated Methane C-H Activation and Functionalization

With protonation and hydride transfer pathways being inconsistent with the relatively mild conditions for conversion of methane to $[CH_3CO]^+$, we then considered the possibility of C-H activation involving an Sb^V-Me intermediate, which could undergo Sb^V to Sb^{III} reduction. The C-H activation transition state involves interaction of the methane C-H bond to the Sb metal center followed by a σ-bond metathesis type transition state **TS4** (Scheme 2c,d) that leads to $[(HF)F_5Sb^V\text{-Me}]^-[H]^+$. Relative to $[Sb^VF_6]^-[H]^+$, the $\Delta G^‡$ for **TS4** is 35.1 kcal mol^{-1} and $\Delta H^‡$ is 26.3 kcal mol^{-1}. The ΔH for forming $[(HF)F_5Sb^V\text{-Me}]^-[H]^+$ is slightly exergonic with ΔG = -7.8 kcal mol^{-1}. Perhaps surprisingly, **TS4** is 5.9 kcal mol^{-1} lower in Gibbs energy and 6.8 kcal mol^{-1} lower in enthalpy compared with **TS3**. In the gas phase the $\Delta\Delta G^‡$ value between **TS4** and **TS3** increases to 18.3 kcal mol^{-1}. Also, comparison of **TS4** and **TS3** at 80 °C and at 34 atm of methane and 19 atm of CO (de Rege conditions) did not significantly change this energy difference. All other functionals and basis sets examined also show that **TS4** is lower in energy than **TS3** (see SI). For example, ωB97X-D/Def2-TZVPDD gave a $\Delta\Delta G^‡_{(\mathbf{TS3}\text{-}\mathbf{TS4})}$ value of 15.0 kcal mol^{-1}. With the viability of **TS4**, we examined several variations. For example, we explored the possibility of a C-H activation transition state from the more reactive $[F_4Sb^V]^+$. However,

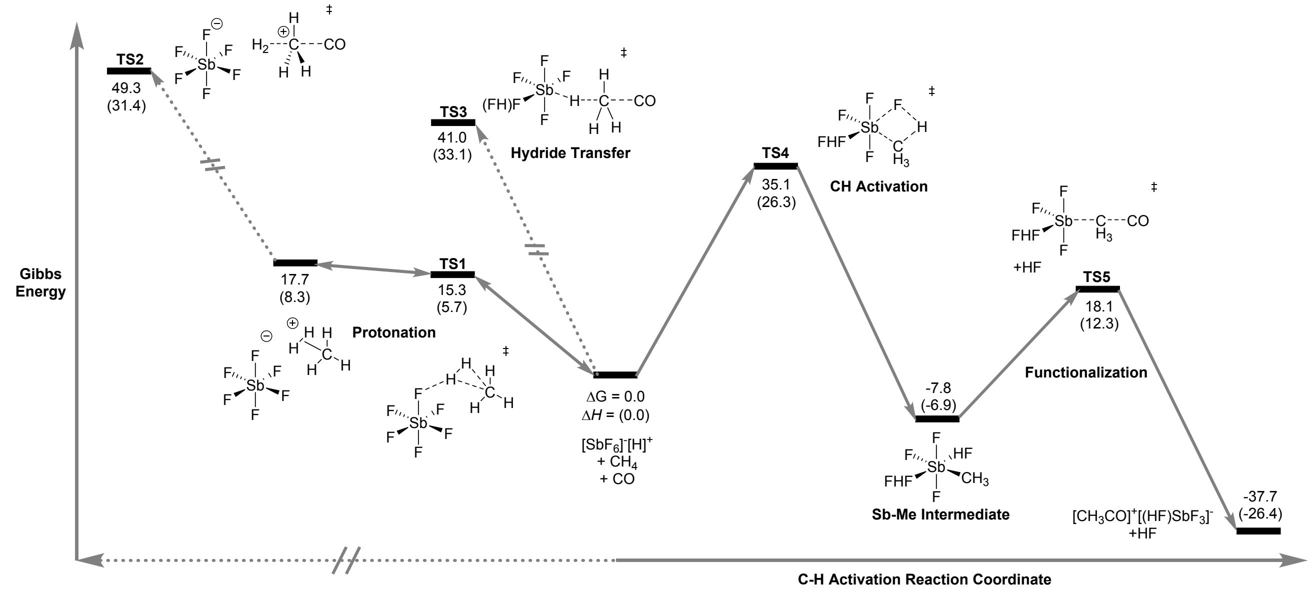

Scheme 3. Energy landscape comparing methane protonation, hydride transfer, and C-H activation reaction pathways for the mononuclear Sb model. Gibbs free energies (enthalpies) in kcal mol^{-1}.

fluoride dissociation is very unfavourable (ΔG = 86.3 kcal mol^{-1}) and while intramolecular fluoride transfer can occur for $Sb^{V}_2F_{10}$, the fluoride bridges and does provide a vacancy around Sb for methane coordination and activation.

Upon C-H activation, a plausible route to $[CH_3CO]^+$ involves Sb^V-Me bond functionalization with CO. We located **TS5** (Scheme 2c,d) where there is displacement of reduced Sb with simultaneous C-C bond formation. The overall reaction thermodynamics leading to $[CH_3CO]^+$ and Sb^{III} is ΔG = -37.7 kcal mol^{-1}. While the Sb^V-Me intermediate is slightly exergonic relative to the starting ground state, which indicates it is potentially observable, the barrier for functionalization is relatively low. The $\Delta G^‡$ for **TS5** is 25.9 kcal mol^{-1} ($\Delta H^‡$ = 19.2) relative to the Sb^V-Me intermediate. This suggest that at the temperature and pressure conditions required to undergo C-H activation that the Sb^V-Me intermediate should rapidly undergo CO functionalization. We also explored alternative Sb^V-Me bond functionalization pathways that were found to be higher in energy. For example, Sb^V-Me bond heterolysis without CO is 24.3 kcal mol^{-1} higher in energy than **TS5** and Sb^V-Me bond homolysis requires >60 kcal mol^{-1}.

With C-H activation and CO functionalization identified as a plausible pathway to explain the observation of $[CH_3CO]^+$ without forming H_2, we continued to examine several other less plausible pathways. For example, we examined the possibility of Sb^VF_5 undergoing reductive elimination to give $Sb^{III}F_3$ and F_2, which could oxidize methane. While the ΔG for this reaction is exergonic, one-step and two-step reductive elimination transition states require transition states with very large barriers ($\Delta G^‡$ >80 kcal mol^{-1}). We also ruled out fluorine and Sb centered radical pathways resulting from Sb-F bond homolysis, which has a bond strength of >80 kcal mol^{-1}.

Dinuclear Sb Model

While the mononuclear Sb model suggests that C-H activation is a lower energy route to methane oxidation than either protonation or hydride transfer pathways, we wondered if a dinuclear Sb model would alter this conclusion. Therefore, we examined these pathways beginning with the ground state model $[Sb^V{}_2F_{11}]^-[H]^+$ (dinuclear bridged $Sb^V{}_2F_{10}$ with HF coordination). Scheme 4 presents the solvent stabilized and gas phase dinuclear pathway energies. The qualitative shape of this dinuclear surface is similar to the mononuclear surface. Again, methane protonation $[Sb^V{}_2F_{11}]^-[H]^+$ leading to the $[Sb_2{}^VF_{11}]^-[CH_5]^+$ ion pair is low in energy, but H_2 dissociation via **TS2** is relatively high in energy at 41.3 kcal mol^{-1}. While this relatively large free energy fits with the experimental lack of H_2 formation, and is close to the experimental barrier for H_2 dissociation from $[CH_5]^+$, the entropy penalty is likely overestimated. Importantly, even though **TS2** is an ion pair, in the gas phase this transition state is significantly higher in energy, with $\Delta G^‡$ = 68.7 kcal mol^{-1} and $\Delta H^‡$ = 50.0 kcal mol^{-1}.

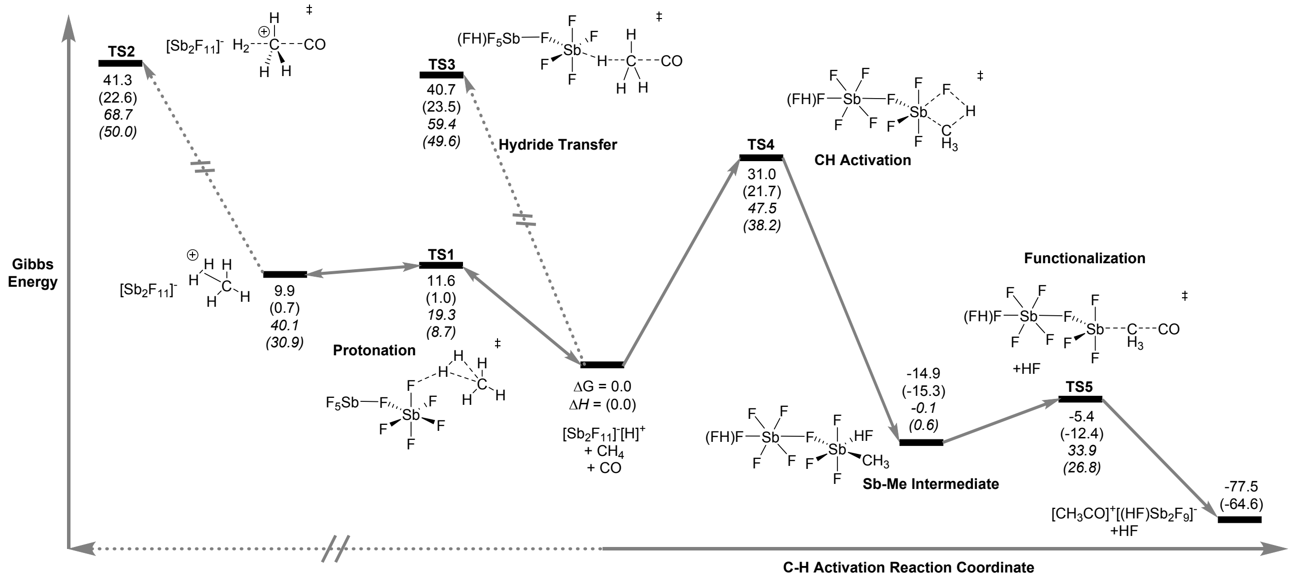

Scheme 4. Energy landscape comparing methane protonation, hydride transfer, and C-H activation reaction pathways for the dinuclear Sb model. Gibbs free energies (enthalpies) in kcal mol^{-1}. Italicized values are gas phase.

Similar to the mononuclear energy surface, the dinuclear hydride and C-H activation transition states are lower in energy than **TS2**. The C-H activation transition state is lower in Gibbs free energy and enthalpy, but only by 2.8 and 2.3 kcal mol^{-1}, respectively. While there remains a clear preference for the C-H activation pathway, the smaller energy difference with the dinuclear model could mean that the hydride pathway may occur as a competitive pathway. In the gas phase, however, as expected due to the lack of stabilization for the charge build up in **TS3**, the C-H activation transition state is lower in Gibbs free energy and enthalpy by more than 10 kcal mol^{-1}. We also examined the relative energies of **TS3** and **TS4** using M06-2X and ωB97X-D functionals. For M06-2X/Def2-TZVPPD and M06-2X/aug-cc-PVTZ the C-H activation transition state **TS4** is lower in Gibbs free energy by 5.3 and 5.7 kcal mol^{-1}, respectively. For ωB97X-D/Def2-TZVPPD and ωB97X-D /aug-cc-PVTZ the C-H activation transition state **TS4** is lower in Gibbs free energy by 5.2 and 5.7 kcal mol^{-1}, respectively. All of these calculations suggest that while hydride transfer could be competitive it would likely contribute in a minor amount to forming $[CH_3CO]^+$. Again, similar to the mononuclear energy surface, while the Sb^V-Me intermediate is slightly exergonic the barrier for functionalization is <10 kcal mol^{-1} on the Gibbs surface and <5 kcal mol^{-1} on the enthalpy surface. However, these very low barriers are due to solvent stabilization of the polarized transition state **TS5**.

Oxidation of Isobutane

As outlined in Scheme 1b, reaction of isobutane with Sb^VF_5 was reported without CO, and results in $Sb^{III}F_3$ with observation of both H_2 and *tert*-butyl cation. While the C-H activation pathway with an Sb^V-R intermediate provides an explanation for the methane oxidation, it is unlikely that C-H activation would result in isobutane oxidation and generate H_2. Therefore, for isobutane, using mononuclear and dinuclear Sb models, we examined protonation and hydride transfer, and compared these pathways to the C-H activation (Scheme 5).

To us, it was surprising that the barrier for protonation of isobutane through **TS6** ($\Delta G^‡$ = 15.2 kcal mol^{-1} and $\Delta H^‡$ = 2.2 kcal mol^{-1} for the dinuclear case, Scheme 5a) is similar to the barrier for methane protonation. However, this is consistent with previous computational results.[5-8] In contrast to the more than 50 kcal mol^{-1} endergonic value to forming methyl cation and H_2 from $[CH_5]^+$, it is exergonic to form *tert*-butyl cation and H_2 from $[C_4H_{11}]^+$. This large energy difference between methane and isobutane results from the wellknown differences between methyl and *tert*-butyl carbocation stability.[36] With $[Sb_2F_{11}]^-$ as a weak assisting nucleophile, there is a low barrier for H_2 dissociation by **TS7** (Scheme 5a).

While there are relatively low barriers for isobutane protonation and H_2 dissociation, there is a lower barrier for hydride transfer. PCET, ET, and HAT have significantly larger barriers or unfavourable thermodynamics compared to hydride transfer (see SI). Relative to $[Sb^V{}_2F_{11}]^-[H]^+$ and isobutane, **TS8** (Scheme 5b) has a $\Delta G^‡$ value of 7.8 kcal mol-1, which is ~26 kcal mol^{-1} lower in energy than **TS3** for methane, and is consistent with the significantly lower hydride affinity of *tert*-butyl cation compared to methyl cation. The ΔG of the anionic Sb^V-H and *tert*-butyl cation ion pair is -20.2 kcal mol^{-1}, which is consistent with its experimental observation.

To confirm that C-H activation is a higher energy pathway than hydride transfer and protonation for isobutane, we calculated **TS9** (Scheme 5c). Although the tertiary C-H bond of isobutane is homolytically weaker than the methane C-H bonds, the C-H activation $\Delta G^‡$ of 40.3 kcal mol^{-1} (Scheme 5, **TS9**) for isobutane is somewhat larger than the barrier for methane, likely due to isobutane repulsion. The slightly larger isobutane C-H activation barrier compared to methane is consistent with Cundari's previous computational study on Co-mediated alkane C-H activation.[37] Because the barrier for C-H activation is relatively insensitive to the alkane structure this allows non-C-H activation pathways to become favored where they are more dramatically influenced by the alkane structure, as is demonstrated here for hydride transfer.

We examined several possible pathways for formation of H_2 after generation of the anionic Sb^V-H, and several plausible pathways emerged. The most viable is by Sb^V-H protonation of isobutane through **TS10** (Scheme 5d). Importantly, the anionic Sb^V-H hydrogen is highly acidic, and we found an extremely low barrier for protonation of isobutane. **TS10** has a $\Delta G^‡$ value of <5 kcal mol^{-1} relative the Sb^V-H intermediate. This protonation also results in Sb^V to Sb^{III} reduction. Generation of H_2 follows by dissociation by **TS7**. This proposed pathway for H_2 formation is consistent with experiments that show that the ratio of H_2 to isobutane is <1.[10-16]

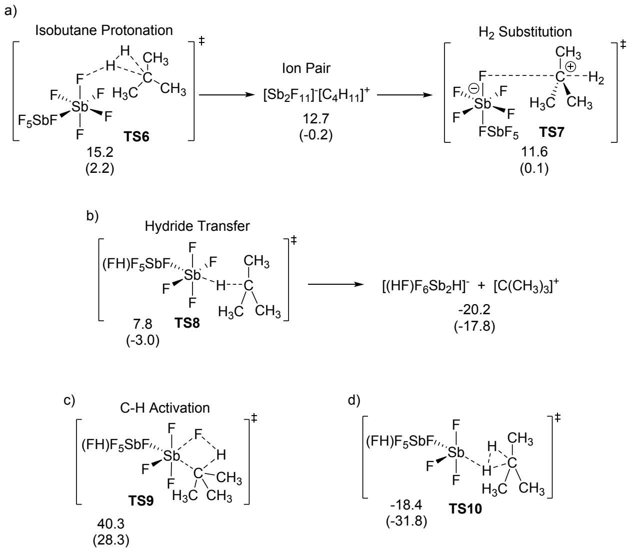

Scheme 5. a) Calculated *tert*-butyl cation pathway that begins with protonation of isobutane. b) Isobutane hydride transfer transition state. c) Isobutane C-H activation transition state. d) Protonation of isobutane by Sb^V-H formed from hydride transfer.

Conclusions

DFT calculations were presented that support a new mechanism for oxidation of methane with Sb^{V}F$_5$. This is the first time that involves C-H activation an organometallic intermediate has been proposed for oxidation of methane by Sb^{V}F$_5$. A low barrier for methane protonation by $[Sb^VF_6]^-[H]^+$ was found, but this pathway is a dead end and reversible because barrier for H_2 dissociation is very large because of the instability of methyl cation. Reversible methane protonation is consistent with the experimentally observed hydrogen-to-deuterium exchange. As a very viable alternative to the methyl cation pathway, the C-H activation/σ-bond metathesis mechanism results in an Sb^V-Me intermediate, which can be functionalized by CO resulting in $[CH_3CO]^+$. In contrast to methane, due to the much lower carbocation hydride affinity, hydride transfer is a much lower pathway for isobutane and results in *tert*-butyl carbocation and H_2 is formed by the resulting Sb^V-H protonation of isobutane.

Conflicts of interest

There are no conflicts to declare.

Acknowledgements

This work was supported by the U.S. Department of Energy, Office of Science, Basic Energy Sciences, Catalysis Science Program, under Award # DE-SC0018329. Funding for Lorna

Suaava was provided by the National Science Foundation Chemistry and Biochemistry REU Site to Prepare Students for Graduate School and an Industrial Career under award CHE-1757627.

Notes and references

1. G. A. Olah, "Electrophilic methane conversion." *Acc. Chem. Res.* **1987**, *20*, 422-428.
2. G. A. Olah, G. Klopman, R. H. Schlosberg, "Super acids. III. Protonation of alkanes and intermediacy of alkanonium ions, penta-coordinated carbon cations of CH_5^+ type. Hydrogen exchange, protolytic cleavage, hydrogen abstraction; polycondensation of methane, ethane, 2,2-dimethylpropane and 2,2,3,3-tetramethylbutane in FSO_3H-SbF_5." *J. Am. Chem. Soc.* **1969**, *91*, 3261-3268.
3. G. A. Olah, Y. Halpern, J. Shen, Y. K. Mo, "Electrophilic reactions at single bonds. III. H-D exchange and protolysis (deuterolysis) of alkanes with superacids. The mechanism of acid-catalyzed hydrocarbon transformation reactions involving the σ electron pair donor ability of single bonds via three-center bond formation." *J. Am. Chem. Soc.* **1971**, *93*, 1251-1256.
4. G. A. Olah, Y. Halpern, J. Shen, Y. K. Mo, "Electrophilic reactions at single bonds. XII. Hydrogen-deuterium exchange, protolysis (deuterolysis), and oligocondensation of alkanes with superacids." *J. Am. Chem. Soc.* **1973**, *95*, 4960-4970.
5. P. M. Esteves, G. G. P. Alberto, A. Ramirez-Solis, C. J. A. Mota, "The alkane σ-bond basicity scale revisited." *J. Am. Chem. Soc.* **1999**, *121*, 7345-7348.
6. P. M. Esteves, A. Ramírez-Solís, C. J. A. Mota, "A Theoretical Study of Alkane Protonation in HF/SbF_5 Superacid System." *J. Braz. Chem. Soc.* **2000**,*11*, 345-348.
7. P. M. Esteves, A. Ramirez-Solis, C. J. A. Mota, "DFT Calculations on the Protonation of Alkanes on HF/SbF_5 Superacids Using Cluster Models." *J. Phys. Chem. B* **2001**, *105*, 4331-4336.
8. P. Dinér, "Superacid-Promoted Ionization of Alkanes Without Carbonium Ion Formation: A Density Functional Theory Study." *J. Phys. Chem. A* **2012**, *116*, 9979-9984.
9. H. Hogeveen, C. J. Gaasbeek, "Chemistry and spectroscopy in strongly acidic solutions. XV. Electrophilic substitution at methane." *Recl. Trav. Chim. Pays-Bas* **1968**, *87*, 319-320.
10. H. Hogeveen, A. F. Bickel, "Formation of trimethylcarbonium ions from isobutane and protons. Basicity of isobutene." *Recl. Trav. Chim. Pays-Bas* **1967**, *86*, 1313-1315.
11. H. Hogeveen, A. F. Bickel, "Chemistry and spectroscopy in strongly acidic solutions. Electrophilic substitution at alkane-carbon by protons." *Chem. Comm.* **1967**, 635-636.
12. G. A. Olah, R. H. Schlosberg, "Chemistry in super acids. I. Hydrogen exchange and polycondensation of methane and alkanes in FSO_3H-SbF_5 ("magic acid") solution. Protonation of alkanes and the intermediacy of CH_5^+ and related hydrocarbon ions. The high chemical reactivity of "paraffins" in ionic solution reactions." *J. Am. Chem. Soc.* **1968**, *90*, 2726-2727.
13. J. C. Culmann, J. Sommer, "Hydrocarbon oxidation by antimony pentafluoride." *J. Am. Chem. Soc.* **1990**, *112*, 4057-4058.
14. J. Sommer, J. Bukala, "Selective electrophilic activation of alkanes." *Acc. Chem. Res.* **1993**, *26*, 370-376.
15. J. Sommer, J. Bukala,; M. Hachoumy, R. Jost, "Reversible Protonation of Isobutane in Liquid Superacids in Competition with Protolytic Ionization." *J. Am. Chem. Soc.* **1997**, *119*, 3274-3279.
16. G. A. Olah, G. K. S. Prakash, Á. Molnár, J. Sommer, Superacid Chemistry, Second Edition, John Wiley & Sons, Inc., Hoboken, New Jersey, **2009**, 511-517.
17. H. Hogeveen, J. Lukas, C. F. Roobeek, "Trapping of the methyl cation by carbon monoxide; formation of acetic acid from methane." *J. Chem. Soc. D* **1969**, 920-921.
18. P. J. F. De Rege, J. A. Gladysz, I. T. Horvath, "Facile and selective carbonylation of methane in superacids." *Adv. Synth. Catal.* **2002**, *344*, 1059-1062.
19. K. Hiraoka, P. Kebarle, "Stabilities and energetics of pentacoordinated carbonium ions. The isomeric protonated ethane ions and some higher analogs: protonated propane and protonated butane." *J. Am. Chem. Soc.* **1976**, *98*, 6119-6125.
20. K. Raghavachari, R. A. Whiteside, J. A. Pople, P. V. R. Schleyer, "Molecular orbital theory of the electronic structure of organic molecules. 40. Structures and energies of C1-C3 carbocations including effects of electron correlation." *J. Amer. Chem. Soc.* **1981**, *103*, 5649-5657.
21. B. G. Hashiguchi, M. M. Konnick, S. M. Bischof, S. J. Gustafson, D. Devarajan, N. Gunsalus, D. H. Ess, R. A. Periana, "Main-Group Compounds Selectively Oxidize Mixtures of Methane, Ethane, and Propane to Alcohol Esters." *Science* **2014**, *343*, 1232.
22. D. Kim, M. L. Klein, "Liquid Hydrogen Fluoride with an Excess Proton: Ab Initio Molecular Dynamics Study of a Superacid." *J. Am. Chem. Soc.* **1999**, *121*, 11251-11252.
23. D. Kim, M. L. Klein, "Ab Initio Molecular Dynamics Study of the Superacid System SbF_5/HF Solution." *J. Phys. Chem. B* **2000**, *104*, 10074-10079.
24. S. Raugei, M. L. Klein, "Structure of the strongly associated liquid antimony pentafluoride: An ab initio molecular dynamics study." *J. Chem. Phys.* **2002**, *116*, 7087-7093.
25. S. Raugei, M. L. Klein, "Hydrocarbon Reactivity in the Superacid SbF_5/HF: an ab Initio Molecular Dynamics Study." *J. Phys. Chem. B* **2002**, *106*, 11596-11605.
26. B. Metz, H. Stoll, M. Dolg, "Small-core multiconfiguration-Dirac–Hartree–Fock-adjusted pseudopotentials for post-d main group elements: Application to PbH and PbO." *J. Chem. Phys.* **2000**, *113*, 2563-2569.
27. D. Rappoport, F. Furche, "Property-optimized Gaussian basis sets for molecular response calculations." *J. Chem. Phys.* **2010**, *133*, 134105.
28. F. Weigend, R. Ahlrichs, "Balanced basis sets of split valence, triple zeta valence and quadruple zeta valence quality for H to Rn: Design and assessment of accuracy." *Phys. Chem. Chem. Phys*. **2005**, *7*, 3297-3305.
29. C. E. Check, T. O. Faust, J. M. Bailey, B. J. Wright, T. M. Gilbert, L. S. Sunderlin, "Addition of Polarization and Diffuse Functions to the LANL2DZ Basis Set for P-Block Elements." *J. Phys. Chem. A* **2001**, *105*, 8111-8116.
30. W. R. Wadt, P. J. Hay, "Ab initio effective core potentials for molecular calculations. Potentials for main group elements Na to Bi." *J. Chem. Phys.* **1985**, *82*, 284-298.
31. K. L. Schuchardt, B. T. Didier, T. Elsethagen, L. Sun, V. Gurumoorthi, J. Chase, J. Li, T. L. Windus, "Basis Set Exchange: A Community Database for Computational Sciences." *J. Chem. Inf. Mod.* **2007**, *47*, 1045-1052. Basis sets were obtained from the basis set exchange: https://www.basissetexchange.org/
32. Gaussian 09, Revision B.01, M. J. Frisch, G. W. Trucks, H. B. Schlegel, G. E. Scuseria, M. A. Robb, J. R. Cheeseman, G. Scalmani, V. Barone, G. A. Petersson, H. Nakatsuji, X. Li, M. Caricato, A. Marenich, J. Bloino, B. G. Janesko, R. Gomperts, B. Mennucci, H. P. Hratchian, J. V. Ortiz, A. F. Izmaylov, J. L. Sonnenberg, D. Williams-Young, F. Ding, F. Lipparini, F. Egidi, J. Goings, B. Peng, A. Petrone, T. Henderson, D. Ranasinghe, V. G. Zakrzewski, J. Gao, N. Rega, G. Zheng, W. Liang, M. Hada, M. Ehara, K. Toyota, R. Fukuda, J. Hasegawa, M. Ishida, T. Nakajima, Y. Honda, O. Kitao,

H. Nakai, T. Vreven, K. Throssell, J. A. Montgomery, Jr., J. E. Peralta, F. Ogliaro, M. Bearpark, J. J. Heyd, E. Brothers, K. N. Kudin, V. N. Staroverov, T. Keith, R. Kobayashi, J. Normand, K. Raghavachari, A. Rendell, J. C. Burant, S. S. Iyengar, J. Tomasi, M. Cossi, J. M. Millam, M. Klene, C. Adamo, R. Cammi, J. W. Ochterski, R. L. Martin, K. Morokuma, O. Farkas, J. B. Foresman, and D. J. Fox, Gaussian, Inc., Wallingford CT, 2016.

33. K. Hiraoka, P. Kebarle, “An application of ion equilibria measurements: Protonated alkanes, protolysis of alkanes and hydride transfer reactions between alkyl cations and alkanes.” *Rad. Phys. Chem. (1977)* **1982**, *20*, 41-49.
34. CYLview, 1.0b; Legault, C. Y., Université de Sherbrooke, 2009 (http://www.cylview.org)
35. G. A. Olah, J. R. DeMember, R. H. Schlosberg, “Friedel-Crafts chemistry. III. Methyl fluoride-antimony pentafluoride, a powerful new methylating agent. Methylation reactions and the polycondensation of methyl fluoride.” *J. Am. Chem. Soc.* **1969**, *91*, 2112-2113.
36. a) See NIST database, https://webbook.nist.gov/. b) C. K. Kim, K. A. Lee, S. Y. Bae, I. S. Han C. K. Kim Bull. Korean Chem. Soc. 2004, 25, 311-313. Hydride affinity values used in this reference are 313 kcal mol^{-1} for methyl cation and 240 kcal mol^{-1} for *tert*-butyl cation. c) Browers, M. T. (e.d.) 1979, Gas Phase Ion Chemistry, Academic Press, New York. d) Values from 36c are also listed in E. V. D. Anslyn, D. A. Dougherty, Modern Physical Organic Chemistry. University Science Books: Sausalito, California, **2006**.
37. a) A. Bakhoda, Q. Jiang, Y. M. Badiei, J. A. Bertke, T. R. Cundari, T. H. Warren, “Copper-Catalyzed C(sp^3)–H Amidation: Sterically Driven Primary and Secondary C–H Site-Selectivity.” *Angew. Chem. Inter. Ed.* **2019**, *58*, 3421-3425. b) S. M. Bellows, T. R. Cundari, W. D. Jones, “Methane Is the Best Substrate for C(sp^3)–H Activation with Cp*(PMe$_3$)Co(Me)(OTf): A Density Functional Theory Study.” *Organometallics* **2015**, *34*, 4032-4038.

Graphical Abstract